ORIGINAL ARTICLE

CrossMark

Phase I metabolic profiling of the synthetic cannabinoids THJ-018 and THJ-2201 in human urine in comparison to human liver microsome and cytochrome P450 isoenzyme incubation

Franziska Gaunitz[1] · Andreas Thomas[2] · Mathias Fietzke[1] · Florian Franz[3,4] · Volker Auwärter[3] · Mario Thevis[2] · Katja Mercer-Chalmers-Bender[1,5]

Abstract

Despite the increasing relevance of synthetic cannabinoids as one of the most important classes within "New Psychoactive Substances", there is still a lack of knowledge concerning their metabolism in humans. Due to the extensive metabolism of synthetic cannabinoids, metabolites are necessarily the best target analytes in urine, posing additional challenges to forensic analysis. The aims of this study were to identify appropriate urinary targets indicating intake of THJ-018 or THJ-2201 as well as to elucidate the most important cytochrome P450 isoenzymes within the metabolism of THJ-018 and THJ-2201 in vitro. For this purpose, the in vitro metabolism of THJ-018 and THJ-2201 was initially established using pooled human liver microsomes. The results obtained were compared to previously published in vitro results as well as to the results of the metabolic profiles from selected recombinant cytochrome P450 isoenzymes and from 23 urine samples from forensic cases. LC-HRMS was used to conduct product ion scans and to examine the metabolite spectra. For THJ-018, 17 different metabolite groups containing 33 different metabolites and isomers were detected after microsomal incubation, with the major metabolic pathways being monohydroxylation at the pentyl chain and of the naphthyl moiety as well as dihydroxylation of both residues. For THJ-2201, 19 different metabolite groups and 46 different metabolites and isomers were observed. The major metabolic pathways were monohydroxylation at the naphthyl moiety and oxidative defluorination. Significant contribution to the in vitro metabolism of THJ-018 and THJ-2201 originated from CYP2B6, CYP2C19, CYP3A4, and CYP3A5. As several cytochrome P450 isoenzymes are involved in the metabolism of these synthetic cannabinoids, a co-consumption with other drugs is unlikely to have an impact on their metabolism.

Keywords Synthetic cannabinoids · THJ-018 · THJ-2201 · Phase I metabolism · Urine · CYP isoforms

Introduction

Synthetic cannabinoids, representing the most prominent substance class within the "New Psychoactive Substances", are subject to extensive metabolism in humans; thus, detection of their intake is challenging and metabolite screening is the only expedient strategy with regard to urine analysis in forensic and clinical laboratories [1]. Despite the continued appearance of

✉ Katja Mercer-Chalmers-Bender
katja.bender@bs.ch

1 Institute of Legal Medicine, Faculty of Medicine, University of Cologne, Melatengürtel 60/62, 50823 Cologne, Germany

2 Institute of Biochemistry, German Sport University Cologne, Am Sportpark Müngersdorf 6, 50933 Cologne, Germany

3 Institute of Forensic Medicine, Medical Center – University of Freiburg, Faculty of Medicine, University of Freiburg, Albertstraße 9, 79104 Freiburg, Germany

4 Hermann Staudinger Graduate School, University of Freiburg, Hebelstraße 27, 79104 Freiburg, Germany

5 Institute of Forensic Medicine, Health Department Basel-Stadt, Switzerland, University of Basel, Pestalozzistrasse 22, 4056 Basel, Switzerland

synthetic cannabinoids, including the appearance of THJ-018 and THJ-2201 some years ago, there is a lack of information on their metabolism.

In contrast to THJ-018 and THJ-2201, in recent years, both the in vitro and in vivo metabolism of their indole templates JWH-018 and AM-2201 has been comprehensively examined utilizing pooled human liver microsomes (pHLM) and hepatic cytochrome P450 isoenzymes (CYPs) assays [1–4] or via the screening of urine samples obtained from forensic and human doping control cases [3, 5–14]. Additional data were provided by using a fungal model (*Cunninghamella elegan*s) [15] and an animal model (Sprague-Dawley rats) [12].

Due to high structural similarity, however, it is likely that their phase I metabolic patterns are very similar. The phase I metabolic pattern of JWH-018 was proven to be monohydroxylation, dihydroxylation, oxidative formation of carbonyl function (here-inafter termed as 'carbonylation') and the carboxylic acid (here-inafter termed as "carboxylation") as well as dihydrodiol formation [2, 4–7, 9–15]. AM-2201 undergoes an additional oxidative dehalogenation exhibiting identical metabolites with JWH-018, namely JWH-018 N-(5-hydroxy pentyl) and JWH-018 N-pentanoic acid (AM-2201 N-pentanoic acid). The formation of JWH-018 N-(4-hydroxy pentyl) is, however, significant for JWH-018 [3, 4, 8, 9, 11–15].

To date, Diao et al. (2015) have published the only in vitro study on the metabolism of THJ-018 and THJ-2201, applying a human hepatocytes assay, which allows the investigation of both phase I and phase II metabolites [16]. The aim of the study presented here was to identify appropriate urinary targets indicating intake of THJ-018 or THJ-2201 and the associated CYPs on the basis of the phase I metabolic patterns obtained by pHLM utilizing in vitro assays. In vitro phase I metabolic patterns of THJ-018 and THJ-2201 were compared to the in vivo findings arising from the screening of 23 authentic urine samples and discussed with respect to the in vitro detected metabolites described by Diao et al. (2015) [16].

Additionally, knowledge of the most important CYP isoforms within the metabolism of a certain drug is of particular interest, due to the possibility of competing drug interactions whenever two or more drugs are administered concurrently (potentially resulting in prolonged activity and elevated toxicity).

Material and methods

Chemicals and reference substances

Solid reference standards of THJ-018 (1-naphthalenyl(1-pentyl-1*H*-indazol-3-yl)-methanone) and THJ-2201 ([1-(5-fluoropentyl)-1*H*-indazol-3-yl]-1-naphthalenyl-methanone) were purchased from Cayman Chemical (Ann Arbor, Michigan, USA). Working solutions (1 mg/mL and 100 μg/mL) were prepared in acetonitrile (ACN). A diazepam stock

solution (1 mg/mL) in methanol (MeOH) was obtained from LGC (Wesel, Germany). For the metabolic activity experiment, 100 μL of the solution was evaporated to dryness under a gentle nitrogen stream and the residue was dissolved in 100 μL ACN.

Analytically pure incubation reagents, namely anhydrous potassium dihydrogen phosphate (KH_2PO_4), magnesium chloride hexahydrate ($MgCl_2 \cdot 6 H_2O$), potassium citrate tri-basic hydrate (cell culture tested), sodium D-glucose-6-phosphate (Glc-6-P), glucose-6-phosphate dehydrogenase (Glc-6-P-DH, EC 1.1.1.49, from *Leuconostoc mesenteroides*, expressed in *Escherichia coli*; 20 U/mL), superoxide dismutase (SOD, EC 1.15.1.1, from bovine erythrocytes), and *β*-nicotinamide adenine dinucleotide phosphate (NADP; sodium salt hydrate, cell culture tested) were purchased from Sigma-Aldrich (Taufkirchen, Germany).

Stock solutions of $MgCl_2$ and Glc-6-P (16.5 mM each) were prepared in ultrapure water, which was generated by a GenPure ultrapure water system (Thermo Fisher Scientific, Dreieich, Germany) and also used for solid phase extraction (SPE). There was 100 mM phosphate buffer (pH 7.4) used to prepare working solutions of NADP (6.5 mM), Glc-6-P-DH (20 U/mL), and SOD (3 kU/mL).

CORNING (Woburn, MA, USA) supplied the pHLM (35-donor pool, including 19 males and 16 females; protein content of 20 mg/mL, total cytochrome P450 content of 300 pmol/mg). Recombinant human CYPs ("Easy Cyp"; expressed in *Escherichia coli*; 1 nmol/mL) 1A2, 2B6, 2C9, 2C19, 2D6, 2E1, 3A4 and 3A5 with low reductase activity were supplied by Cypex (Scotland, UK) via tebu-bio (Offenbach, Germany).

HPLC gradient grade acetone and Ultramark® 1621 were purchased from Alfa Aesar (Karlsruhe, Germany). MRFA (a tetra-peptide consisting of methionine, arginine, phenylalanine and alanine) was obtained from Research Plus (Bayonne, IL, USA). LC-MS grade ACN, MeOH and water were purchased from Carl Roth (Karlsruhe, Germany). LC-MS grade formic acid and the caffeine standard for high resolution mass spectrometry (HRMS) were obtained from Sigma Aldrich (Taufkirchen, Germany).

β-Glucuronidase (*β*-D-glucuronoside glucuronoso-hydro-lase, EC 3.2.1.31, from *Escherichia coli* K12; 140 U/mL) was obtained from Roche Diagnostics (Mannheim, Germany).

SPE cartridges (Empore™ Disk Cartridge C18 SD, 7 mm/3 mL) were purchased from 3 M (St. Paul, MN, USA).

Microsomal incubation

The microsomal incubation approach was based on Wintermeyer et al. (2010) [2] and Fietzke et al. (2016) [17], and on manufac-turer's (CORNING) recommendations. As modifications regard-ing the concentrations of NADP and substrate and incubation time were not proven to generate higher metabolite abundancies or additional metabolites, the approach's conditions were retained. A total assay volume of 250 μL was prepared by

mixing 30 μL of 100 mM phosphate buffer (pH 7.4), 50 μL MgCl$_2$ (3.3 mM final concentration), 50 μL NADP (1.3 mM final concentration), 50 μL Glc-6-P (3.3 mM final concentration), 20 μL Glc-6-P-DH (1.6 U/mL final activity), 20 μL SOD (240 U/mL final activity), and 10 μL of the synthetic cannabinoid (0.11 μM final concentration; 4% final organic solvent proportion). The reaction was initiated by addition of 20 μL pHLM (1.6 mg/mL final concentration) and vortexing.

The incubation, performed at physiological temperature (37 °C) in a gently shaking (700 rpm) Thermomixer 5436 (Eppendorf, Hamburg, Germany), was stopped after 3 h by addition of 250 μL of ice-cold ACN. The samples were subsequently stored in a freezer (− 20 °C) for 10 min to reinforce the precipitation, after which they were centrifuged for 10 min at 4 °C and 9000×g in a Heraeus Fresco 17 centrifuge (Thermo Scientific, Waltham, Massachusetts, USA). The obtained supernatants then underwent a SPE clean-up.

Metabolic activity

To verify metabolic activity of the microsomal incubation assay, diazepam was incubated with pHLM (0.14 μM final concentration).

Metabolic stability

To examine the metabolic stabilities of THJ-018 and THJ-2201, a total assay volume of 2 mL was prepared for each substance by mixing the eightfold volume of the assay ingredients. The reaction was finally initiated by addition of 160 μL pHLM and vortexing. An aliquot of 250 μL was immediately removed and the reaction was stopped by addition to 250 μL of ice-cold ACN. Further 250 μL samples were taken after 15 min, 30 min, 45 min, 1 h, 2 h, and 3 h and added to 250 μL ice-cold ACN. The reaction in the remaining 250-μL aliquot was stopped after 4 h, as an additional sample.

CYP incubation

Incubation with selected CYPs was carried out analogous to the microsomal incubation. Separate experiments for each CYP isoform were initiated by addition of 20 μL enzyme (80 pmol/mL final concentration) following the addition of 10 μL of the synthetic cannabinoid (0.01 μM final concentration).

Blank and negative control samples

Drug-free blanks were prepared with ACN replacing the synthetic cannabinoid standard solution. Negative controls were prepared by replacing pHLM or CYP by phosphate buffer, respectively. Blank and negative control samples were incubated in order to detect matrix interferences.

Processing of authentic human urine samples

The metabolite screening was applied to 23 authentic urine samples from cases, provided by the Institute of Forensic Medicine Freiburg. Urine samples were from 11 proven THJ-018 users (including 10 males and one female) and 12 urine samples originated from proven THJ-2201 users (all male). A 500-μL aliquot of each urine sample was incubated with 10 μL β-Glucuronidase in order to cleave glucuronides into the corresponding phase I metabolites. Incubation was performed for 1 h at 37 °C using the Thermomixer 5436, and was based on the procedure for the hydrolysis of β-glucuronides provided by the manufacturer which was validated for various in-house methods and analytes. However, due to a lack of available reference standards, a substance-specific validation of the glucuronide cleavage was not carried out. Thus, a total cleavage of glucuronides cannot be fully guaranteed.

Automatic solid-phase extraction (SPE)

SPE was carried out on a GILSON GX-274 ASPEC™ (Middleton, USA). Prior to SPE, 400 μL supernatant from the incubation samples and 200 μL of the treated authentic urine samples were transferred into glass tubes and diluted with 1600 μL and 1800 μL ultrapure water, respectively. Diluted samples were loaded onto the cartridges following the condition with 2 mL each of MeOH and ultrapure water. To avoid carry-over, the automated SPE system was rinsed three times with an acetone/ultrapure water mixture (90/10; v/v) between the loading and washing step, in which cartridges were washed twice with 1 mL ultrapure water in order to remove matrix components. Subsequently, the cartridges were dried with nitrogen for 5 min. Elution of the analytes was carried out by twice loading 1 mL ACN onto the cartridges. Eluates were collected in 5-mL glass tubes and evaporated to dryness under a gentle nitrogen stream at 40 °C utilizing a Vapotherm evaporator (Barkey, Leopoldshöhe, Germany). The dried residues were dissolved in 50 μL ACN, transferred into HPLC vials (N9, flat, screw neck, 1.5 mL, 11.6 × 32 mm, clear; Macherey-Nagel, Düren, Germany) with inserts (15 mm tip, wide opening, 0.2 mL, 6 × 31 mm, clear; Macherey-Nagel, Düren, Germany) and stored at − 20 °C until LC-HRMS analysis. SPE washing solutions were not screened for THJ-018 and THJ-2201 metabolites, respectively.

With respect to the metabolic activity verification with diazepam, screening for diazepam metabolites was conducted using a validated in-house LC-ESI-MS/MS method for benzodiazepines and metabolites. Based on the associated SPE protocol, each 100 μL supernatant of the

incubation samples was diluted with 2000 μL 150 mM phosphate buffer (pH 6) and subsequently extracted utilizing strata-x-drug B cartridges (60 mg/3 mL; 33 μm) from Phenomenex (Torrance, CA, USA). Chromatographic separation was achieved using a Nucleoshell C18 column (2.0 × 150 mm; 2.7 μm particle size) from Macherey Nagel (Düren, Germany).

LC-HRMS conditions

LC-HRMS experiments were conducted on a Dionex™ UltiMate 3000 LC system coupled to a Thermo Scientific™ Q Exactive™ plus from Thermo Fisher Scientific (Bremen, Germany), which is a Fourier transform mass spectrometer (FTMS), equipped with a heated electrospray ionization (HESI-II) source and a hybrid-quadrupole-orbitrap.

The LC system consisted of an LPG-3400XRS pump, a TCC-3000 column oven and an OAS-3000 open auto-sampler. Chromatographic separation was performed at ambient temperature on a Hypersil GOLD™ C18 column (2.1 × 50 mm; 1.9 μm particle size) from Thermo Fisher Scientific.

The mobile phase consisted of 0.1% formic acid in both water (solvent A) and ACN (solvent B). Initial conditions were 15% of solvent B held for 5 min, subsequently increasing to 60% within 1 min and then to 99% within 1 min. After 7 min run time, the system was returned to initial conditions and held for a further 3 min. Total run time was 10 min. Chromatographic conditions were proved to be sufficient for both the separation of THJ-018 and THJ-2201 metabolites, and to cover the parents. The auto-sampler temperature was set to 10 °C and the flow rate was set to 0.250 mL/min. The injection volume was 10 μL.

The source was operated in positive ionization mode at an ion spray voltage of 4000 V and a capillary temperature of 300 °C. Nitrogen, provided by a nitrogen generator from CMC Instruments (Eschborn, Germany), was used as the collision gas. Full MS data were collected over a scan range of [m/z] 100 to 1000 and at a resolution of 30,000 full width at half maximum (FWHM). Up to five targeted MS/MS experiments were conducted simultaneously in the product ion monitoring (PRM) mode. Targeted MS/MS data were acquired at a resolution of 15,000 FWHM. The Automatic Gain Control (AGC) target was set to 3e6 for both experiments. For targeted MS/MS experiments, the isolation window of the quadrupole was set to [m/z] 1.5. The stepped normalized collision energy (NCE) [%] was operated at 20, 40, and 60. To examine the fragmentation pattern of THJ-018 and THJ-2201, higher collision dissociation (HCD) was performed at NCE [%] of 10, 20, 30, 50, and 70. HRMS parameters were optimized for the parent compounds and applied for

subsequent product ion scan (PIS) in order to detect THJ-018 and THJ-2201 metabolites. PIS were based on published data referring to the metabolism of JWH-018 and AM-2201, THJ-018 and THJ-2201, and synthetic cannabinoids in general (see "Introduction"). To ensure mass accuracies < 5 ppm, the HRMS was calibrated using standard solutions of caffeine, MRFA and Ultramark® 1621.

Postulated product ions and their calculated monoisotopic masses, which were determined using ChemSketch (Version 2015, ACD Labs), are presented in Table 1.

Results

Metabolic activity

The metabolic activity of the pHLM assay was proven by the detection of nordiazepam, temazepam, and oxazepam. The loss of diazepam was approximately 20% after 3 h incubation. The relative concentrations compared to diazepam were 12%, 54%, and 1%, respectively.

Metabolic stability

THJ-2201 was proven to be rapidly metabolized by pHLM. The loss of the parent compound was approximately 25% after 30 min and 50% after 1 h, respectively, with only 30% remaining after 3 h. In contrast, THJ-018 seemed to be more stable compared to THJ-2201, as the loss of parent compound was approximately only 20% after 3 h incubation.

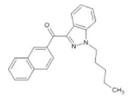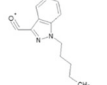### Collision-induced dissociation of THJ-018 and THJ-2201
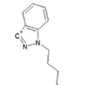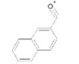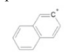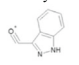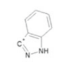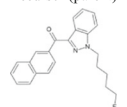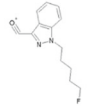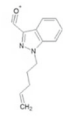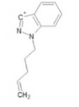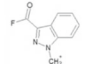
HR product ion mass spectra of THJ-018 and THJ-2201 were recorded from precursor ions found at [m/z] 343 and [m/z] 361, respectively (see Table 1). The dominant product ion was the indazole acylium fragment ion [m/z] 145. The indazole fragment ion [m/z] 117 was only observed for THJ-018. Both THJ-018 and THJ-2201 gave rise to the naphthalene acylium fragment ion [m/z] 155 and the naphthalene fragment ion [m/z] 127 as well.

Another common product ion, [m/z] 215 for THJ-018 and [m/z] 233 for THJ-2201, may originate from the neutral loss of the naphthalene moiety. Further neutral loss of hydrogen fluoride (− 20 Da) from [m/z] 233 led to [m/z] 213.

Metabolic pattern of THJ-018 after incubation with pHLM

Microsomal incubation of THJ-018 yielded 33 metabolites, belonging to eight different main groups (M01–

Table 1 Proposed product ion structures of THJ-018 and THJ-2201 along with molecular formulae, calculated and measured accurate mass values and mass accuracies, and of product ions referring to their predicted metabolites

[m/z]	Product ion structure	Molecular formula	[M+H]⁺	[M+H]⁺ (accurate mass)	Mass accuracy (ppm)	OH	C=O	(OH)₂	Dihydrodiol	COOH	(OH)₃
THJ-018	Precursor (parent)	$C_{23}H_{22}N_2O$	–	343.1801	–	359.1754	357.1598	375.1703	377.1860	373.1547	391.1652
	Indazole acylium ion + pentyl chain	$C_{13}H_{15}N_2O$	215.1178	215.1178	−0.4030	231.1128	229.0971	247.1077	–	245.0921	263.1026
	Indazole ion + pentyl chain	$C_{12}H_{15}N_2$	–	187.1230	–	203.1179	201.1022	219.1128	–	217.0972	235.1077
THJ-018 and THJ-2201	Naphthalene acylium ion	$C_{11}H_7O$	155.0491	155.0697	−0.0234	171.0441	–	187.0390	189.0546	–	–
	Naphthalene ion	$C_{10}H_7$	127.0542	127.0542	−0.3680	143.0491	–	159.0441	161.0597	–	–
	Indazole acylium ion	$C_8H_5N_2O$	145.0396	145.0396	−0.0275	161.0346	–	177.0295	–	–	–
	Indazole ion	$C_7H_5N_2$	117.0449	117.0445	1.8797	133.0396	–	149.0345	–	–	–
	Precursor (parent)	$C_{23}H_{21}FN_2O$	–	361.1709	–	377.1660	–	393.1609	395.1765	373.1547	–
THJ-2201	Indazole acylium ion + 5-fluoropentyl chain	$C_{13}H_{14}FN_2O$	233.1084	233.1084	−0.3770	249.1034	247.0877	265.0983	–	245.0921	–
	Indazole acylium ion + pent-4-en-1-yl chain (loss of hydrogen fluoride)	$C_{13}H_{13}N_2O$	213.1021	213.1022	−0.0973	229.0971	227.0815	245.0921	–	–	–
	Indazole ion + pent-4-en-1-yl chain (loss of hydrogen fluoride)	$C_{12}H_{13}N_2$	185.1074	185.1074	0.0664	201.1022	–	217.0972	–	(217.0971)	–
	3-fluorocarbonyl indazole methylium ion	$C_9H_6FN_2O$	177.0458	177.0459	1.0974	193.0408	–	–	–	–	–

M08) and 17 subgroups, respectively, which are described in detail below and summarized in Supplementary Table 1. No interfering signals were observed in the blank and negative control samples.

Monohydroxylation (M01)

Eight monohydroxylated metabolites of THJ-018 were identified by product ion screening of the precursor ion [m/z] 359. The PIS of M01.1 (monohydroxylation of the naphthyl moiety) was characterized by product ions [m/z] 215, 145 and 117, representing an unaltered indazole and pentyl moiety. The presence of the product ion at [m/z] 171 indicated a monohydroxylated naphthalene acylium moiety. The M01.1 metabolite was one of the most abundant metabolites and detected four times.

The PIS of M01.2 and M01.3 displayed the ions at [m/z] 155 and 127 as well as [m/z] 231, indicating an unaltered naphthyl moiety and a monohydroxylation of the indazole or pentyl moiety. M01.2 (monohydroxylation of the indazole moiety) was identified as the characteristic ions at [m/z] 161 and 133 were observed. The M01.2 metabolite was only detected once. In the case of M01.3 (monohydroxylation of the aliphatic side chain), the detection of [m/z] 145 and 117 indicated a non-altered indazole moiety and monohydroxylation of the pentyl chain. This was confirmed by the detection of [m/z] 213 according to a neutral loss of water from [m/z] 231 (-18 Da) during ionization. The M01.3 metabolite was detected three times and showed, along with the M01.1 metabolite, the highest peak intensities. In addition, the M01.3 metabolite, eluted after 6.9 min, was presumed to be the THJ-018 N-(5-OH-pentyl) metabolite as an identical metabolite of THJ-018 and THJ-2201 due to the detection of the F04.1 metabolite, matching retention time (see Fig. 1), mass spectra and product ion ratios. Monohydroxylation in the ω-position to N-(5-OH-pentyl) has already been reported as a common metabolite of synthetic cannabinoids with a pentyl chain along with its 5F-pentyl analogue in the literature [2, 3, 7–16]. Furthermore, monohydroxylation in the ω-1-position to N-(4-OH-pentyl) was reported to be a relevant monohydroxylation of the aliphatic side chain [1, 4, 16, 18].

Dihydroxylation (M02)

For the elucidation of dihydroxylated metabolites, a PIS of [m/z] 375 was conducted resulting in the detection of 12 metabolites. M02.1 (dihydroxylation of the naphthyl moiety) was the only dihydroxylated metabolite type which displayed the [m/z] 215 fragment, correlating with an unchanged indazole moiety and aliphatic side chain. The bearing of both hydroxyl groups at the naphthyl moiety was indicated by the detection of [m/z] 187 and 159. The M02.1 metabolite was detected three times. Mass spectra of M02.2 and M02.5 shared [m/z] 155 and 127 as well as [m/z] 247, suggesting an unaltered naphthyl moiety and a dihydroxylation at the N-pentyl-3-carboxyindole moiety. M02.2 (dihydroxylation of the pentyl chain) could be assigned due to the detection of [m/z] 145 and 117. Mass spectra of M02.5 displayed not only [m/z] 247, but

also [m/z] 161, suggesting a monohydroxylation of each indazole and pentyl moiety. The M02.2 metabolite was detected once, while M02.5 was detected twice. Monohydroxylation of the naphthyl moiety in M02.3 and M02.4 was determined by the detection of [m/z] 171. The [m/z] 143 was only detected for M02.3. M02.3 and M02.4 also shared [m/z] 231, suggesting an additional monohydroxylation of the indazole or pentyl moiety. The mass spectrum of M02.3 contained [m/z] 161 and [m/z] 133, suggesting an additional monohydroxylation of the indazole moiety. These fragments were not observed for M02.4 suggesting the additional monohydroxylation being located at the alkyl moiety. One M02.3 metabolite and five M02.4 metabolites were detected after microsomal incubation. Apart from the M0.1 and M01.3 metabolites, M02.4 (dihydroxylation at the naphthyl moiety and the aliphatic side chain) exhibited comparably high abundancies.

Trihydroxylation (M03)

Five threefold hydroxylated metabolites were identified by occurrence of diagnostic product ions in the corresponding MS/MS experiments at [m/z] 391. Mass spectra of M03.1 (dihydroxylated aliphatic side chain along with a monohydroxylated naphthyl moiety) contained a product ion at [m/z] 171, suggesting a monohydroxylation at the naphthyl moiety. Dihydroxylation of the pentyl residue was indicated by [m/z] 247, 145 and 117. M03.1 was detected four times. In addition, one M03.2 metabolite (monohydroxylated aliphatic side chain along with a dihydroxylation at the naphthyl moiety) was detected. Its mass spectrum revealed [m/z] 117, 145 and 231 as well as [m/z] 159 and 187.

Monohydroxylated metabolites with additional carbonyl function and pentanoic acid (M04)

PIS of [m/z] 373 included metabolites which underwent monohydroxylation at the aliphatic side chain in ω- or ω1-position and further oxidation to a carbonyl function leading to an aldehyde or ketone, respectively, along with a second monohydroxylation. PIS of [m/z] 373 also included the pentanoic acid and yielded, in total, four metabolites.

The spectra of the two M04.1 metabolites contained [m/z] 171 due to a monohydroxylated naphthyl moiety and [m/z] 229, 145 and 117, indicating an unaltered indazole moiety and a carbonyl function. The spectrum of M04.2, detected once, contained [m/z] 161 and 133 due to a monohydroxylated indazole moiety. Mass spectra of M04.1 and M04.2 shared [m/z] 85 as a common fragment ion and may be related to an elimination of a methyl residue (-14 Da) from the aliphatic side chain with a carbonyl function, but the origin of this fragment ion remains unclear. Moreover, M04.2 shared product ions with M04.3, in particular, at [m/z] 245, 155 and 127,
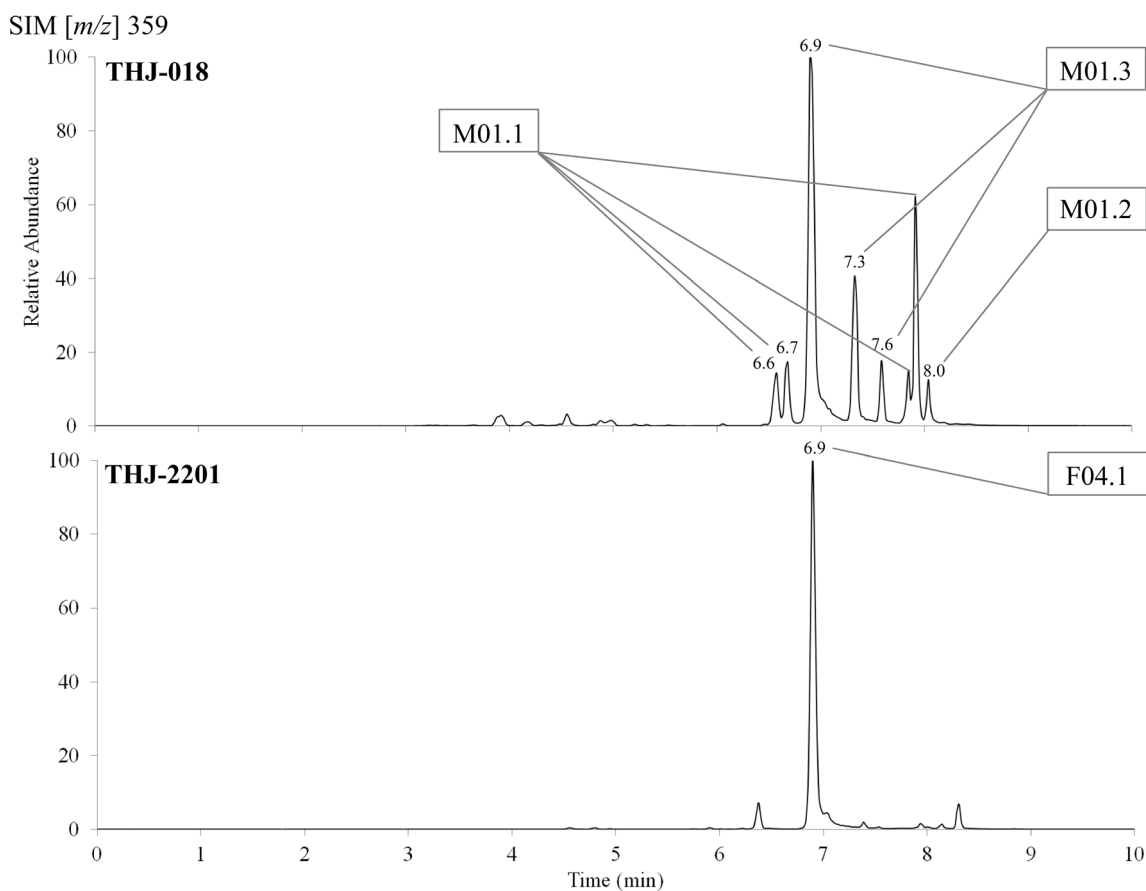
Fig. 1 Chromatograms of the product ion scan of [*m/z*] 359 of THJ-018 and THJ-2201 after incubation with pHLM

indicating monohydroxylation and carbonylation at the 1-pentyl-3-carboxyindazole moiety along with an unaltered naphthyl moiety. In contrast to M04.2, the M04.3 spectrum additionally contained [*m/z*] 145 and 117, suggesting an unaltered indazole moiety. Due to the detection of [*m/z*] 327, indicating a neutral loss of formic acid (− 46 Da), M04.3 was finally assumed to be the THJ-018 N-pentanoic acid. This conclusion was reached on consulting data from the literature, as the pentanoic acid is reported to be a further mutual metabolite of synthetic cannabinoids and their 5F-pentyl analogues [1–3, 7–16, 18] - confirmed by the detection of the F07.1 (THJ-2201 N-pentanoic acid) metabolite after microsomal incubation of THJ-2201 (see Fig. 2).

Formation of dihydrodiol-function (M05)

Formation of dihydrodiol-function was identified by PIS of precursor ion [*m/z*] 377. The mass spectrum of M05.1 contained product ions at [*m/z*] 215, 145 and 117, indicating both an unaltered indazole moiety and aliphatic residue. Due to the simultaneous detection of [*m/z*] 189 and 171, the formation of a dihydrodiol-function located at the naphthyl moiety was assumed.

Metabolic introduction of a carbonyl function (M06)

A metabolite with a carbonyl function at the pentyl chain could be identified via PIS of the precursor ion [*m/z*] 357. The mass spectrum of M06.1 showed [*m/z*] 229, 145 and 85, which had already been detected for M04.1, and also featured a carbonyl function at the pentyl chain and an unaltered indazole moiety. In addition, the [*m/z*] 155 was observed, confirming the assumption.

Dehydrogenation (M07)

Dehydrogenation was observed by PIS of precursor ion [*m/z*] 341. M07.1 shared [*m/z*] 213, 155 and 145, indicating both an unaltered indazole and naphthyl moiety, as well as a double bound at the pentyl chain due to a conceivable metabolic elimination of water after monohydroxylation.

N-Desalkylation (M08)

PIS of precursor ion [*m/z*] 273 revealed the existence of metabolite M08.1, following N-desalkylation of THJ-018. Its

SIM [m/z] 373
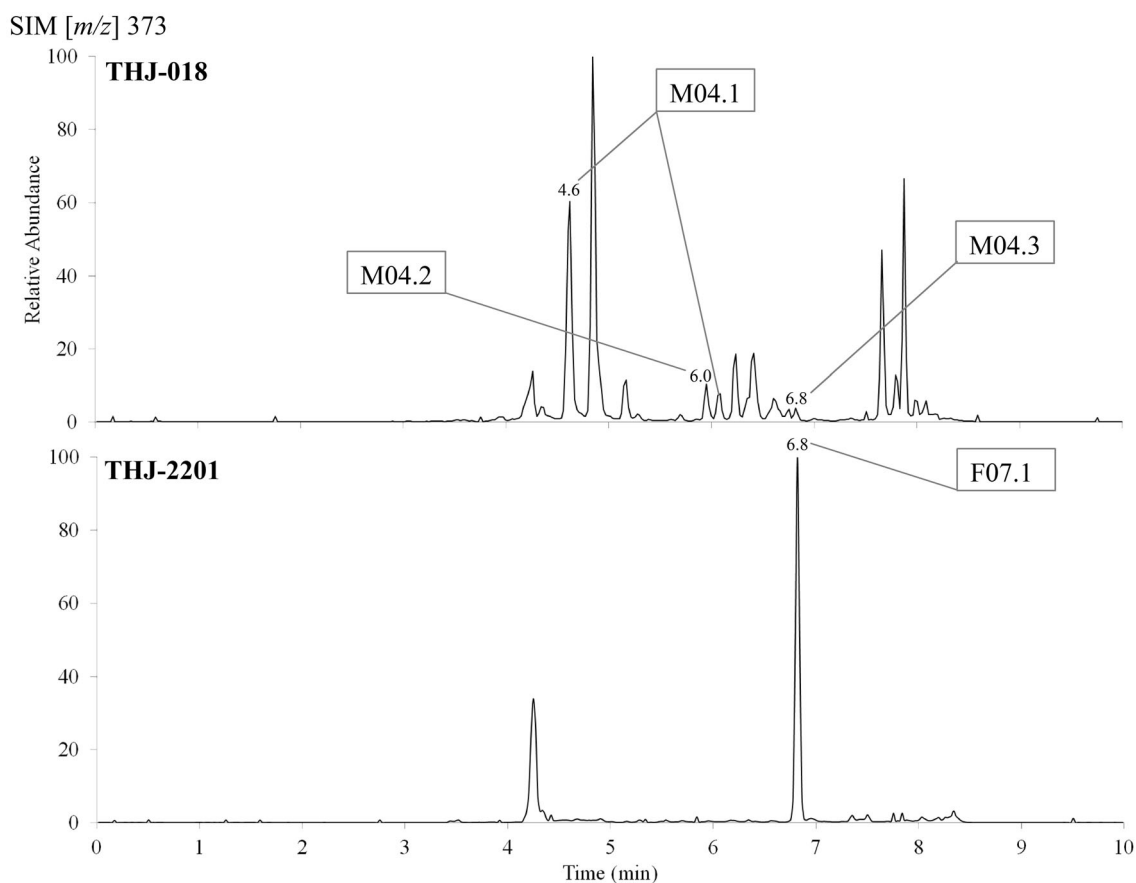
Fig. 2 Chromatograms of the product ion scan of [m/z] 373 of THJ-018 and THJ-2201 after incubation with pHLM

mass spectrum contained [m/z] 145 and 117, indicating a desalkylated indazole moiety.

Metabolic pattern of THJ-018 after incubation with CYPs

With regard to metabolite subgroups, CYP incubation delivered approximately the half of the identified THJ-018 metabolites identified after microsomal incubation (see Supplementary Table 1). In total, the number of THJ-018 metabolites detected after CYP incubation ranged between four (CYP2E1) and 10 (CYP2C19) metabolite types. With respect to their summed metabolite peak abundancies, CYP3A4, CYP2C19, CYP2B6, and CYP3A5 were observed to contribute most to the microsomal metabolism of THJ-018 (listed here in the order of relevance), followed by CYP2C9, CYP2D6, and CYP1A2. CYP2E1 made, by far, the lowest contribution.

Comparison of in vitro THJ-018 metabolic patterns with in vivo metabolic patterns

Table 2 provides a comparison of in vitro metabolic patterns of THJ-018 obtained after pHLM and CYP incubation, as well as those obtained from hepatocyte incubation as reported by Diao et al. (2016) [16] with in vivo metabolic patterns obtained via application of the THJ-018 metabolites screening method to 11 urine samples from authentic cases. Figure 3 provides a final overview of the metabolic pathways of THJ-018 postulated after incubation with pHLM. Metabolites which were detected in the authentic urine samples from proven THJ-018 users are printed in bold and labelled with the CYP isoenzymes which were proven to catalyze the metabolic reactions.

Compared to Diao et al. (2015) [16], results were in good accordance, with some exceptions. Microsomal incubation yielded far more metabolites and shared only one main metabolite with hepatocyte incubation, namely M01.3 (monohydroxylation at the aliphatic side chain) being identical with M8 – M10 (as abbreviated in the reference), respectively. However, metabolites detected in urine could be observed with almost all of the in vitro models. Although M02.4 was not observed after CYP2B6 and CYP2E1 incubation, evaluation of the results showed that all three in vivo observed metabolites was produced by various CYPs and that no metabolite is produced by a single CYP alone.

Table 2 Detected THJ-018 metabolites after pHLM and CYP incubation in comparison with metabolites from human urine samples and metabolites after incubation with human hepatocytes, as reported by Diao et al. (2015) (the three most abundant in vitro metabolites per assay are highlighted)

Metabolites		Metabolic reaction			Human urine (n = 11)	pHLM	CYP								Human hepatocytes (abbreviations used in the reference) [16]
	Abbreviation	i	a	n			1A2	2B6	2C9	2C19	2D6	2E1	3A4	3A5	
M01 OH	M01.1			OH		☒	☒	×	×	×	☒	×	×	☒	
	M01.2	OH				×	☒	×	☒	×					
	M01.3		OH		☒ (n = 8)	☒	☒	☒	☒	☒	☒	☒	☒	☒	☒ (M8, M9, M10)
M02 (OH)₂	M02.1			(OH)₂		×	×			×	×		☒	×	
	M02.2		(OH)₂			×									
	M02.3	OH		OH		×									
	M02.4		OH	OH	× (n = 2)	☒	×		×	☒	☒		☒	☒	× (M1)
	M02.5	OH				×									
M03 (OH)₃	M03.1	(OH)₂		OH		×									
	M03.2		OH	(OH)₂		×									
M04 C=O + OH or COOH	M04.1		C=O	OH		×				×			×	×	× (M2)
	M04.2	OH	C=O			×		×		×					
	M04.3		COOH			×				×					× (M7)
M05 dihydrodiol	M05.1			dihydrodiol		×	×	×			×		×	×	× (M6)
M06 C=O	M06.1		C=O			×	×	☒	×	☒	×	☒	×	×	☒ (M11, M12)
M07 C=C	M07.1		C=C		× (n = 4)	×	×	☒	☒	×	×	☒	×	×	☒ (M13)
M08 N-desalkylation	M08.1	N-desalkylation				×	×	×					×	×	× (M5)

i indazole moiety

a aliphatic side chain

n naphthyl moiety

OH monohydroxylation

(OH)₂ dihydroxylation

(OH)₃ trihydroxylation

C=O "carbonylation" (formation of a carbonyl function)

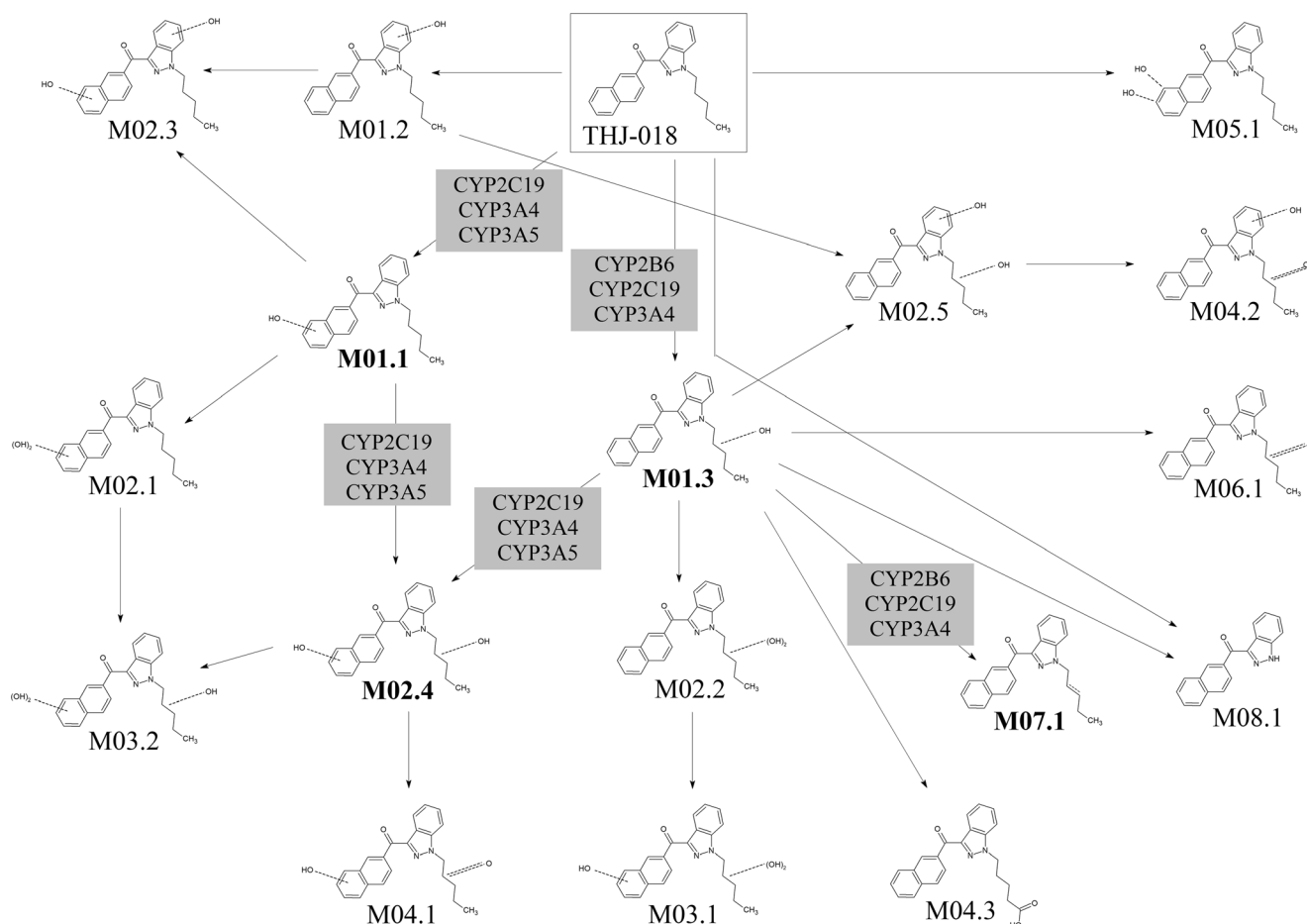*COOH* "carboxylation" (formation of the pentanoic acid)

Fig. 3 Postulated metabolic pathways of THJ-018 after incubation with pHLM. Metabolite types detected in urine samples from THJ-018 users are printed in bold type and labelled with the CYP isoforms that dominantly catalyzed the reactions

In addition, according to main in vitro observed metabolites hepatocyte incubation yielded a better match compared to in vivo observed metabolites.

With regard to the urine screenings, eight out of 11 samples from proven THJ-018 users were tested positive for M01.3, five samples were demonstrated to be positive for M07.1 (metabolite with a monounsaturated pentyl chain) and two were tested positive for M02.4 (monohydroxylation at both the aliphatic side chain and at the naphthyl moiety).

Metabolic pattern of THJ-2201 after incubation with pHLM

In total, microsomal incubation of THJ-2201 yielded 46 metabolites, belonging to nine different main groups (F01–F09) and 19 subgroups, respectively. Examinations are described in detail in the following paragraphs and tabulated in Supplementary Table 2. No interfering signals were observed in the blank and negative control samples.

Monohydroxylation (F01)

In total, nine monohydroxylated metabolites of THJ-2201 could be identified by PIS of precursor ion [m/z] 377.

Mass spectra of F01.1 (monohydroxylation of naphthyl moiety) and F01.3 (monohydroxylation of the aliphatic side chain) shared [m/z] 177, 145 and 117 due to an unaltered indazole residue. The additional observation of [m/z] 233, 213 and 185 as well as of [m/z] 171 in the mass spectrum of F01.1 suggested an unaltered 1-(5F-pentyl)-1H-indazole moiety and a monohydroxylation of the naphthyl moiety, respectively. In addition, [m/z] 213 and 185 originated from a neutral loss of hydrogen fluoride during ESI fragmentation. F01.1 was one of the main THJ-2201 metabolites as well as the most common monohydroxylated THJ-2201 metabolite, giving rise to five peaks in the chromatogram (see Fig. 4).

Moreover, [m/z] 155 and 127 were observed for the F01.2 metabolite and the F01.3 metabolites, suggesting an unaltered naphthyl moiety. Their spectra also contained [m/z] 249 and 229, indicating a monohydroxylation of the 1-(5F-pentyl)-1H-
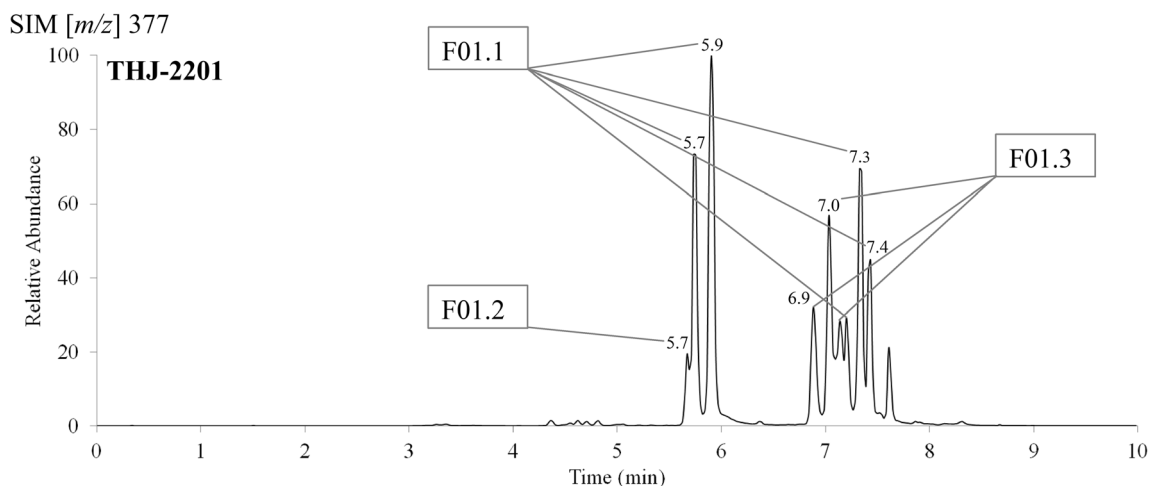
Fig. 4 Chromatogram of the product ion scan of [*m/z*] 377 of THJ-2201 after incubation with pHLM

indazole moiety. The mass spectrum of F01.2 also contained [m/z] 201, whereby [*m/z*] 229 and 201 both originated from the neutral loss of hydrogen fluoride (− 20 Da) from [*m/z*] 249.

The mass spectrum of F01.2 further displayed [*m/z*] 193, 161 and 133 due to a monohydroxylation of the indazole moiety. The F01.2 metabolite was detected once.

The detection of [*m/z*] 231 in the mass spectrum of F01.3 was due to a neutral loss of water (− 18 Da) from [*m/z*] 249, indicating a monohydroxylation at the 5-fluoropentyl chain. F01.3, one of the most abundant THJ-2201 metabolites, was detected three times.

Dihydroxylation (F02)

Fourteen dihydroxylated species of THJ-2201 were examined by PIS of precursor molecule ion [*m/z*] 393.

The mass spectra of F02.1 and F02.3 shared [*m/z*] 177, 145 and 117, indicating an unaltered indazole moiety. The mass spectra of the four F02.1 (dihydroxylation of the naphthyl moiety) metabolites additionally contained [*m/z*] 233, 213 and 185, indicating an unaltered 5F-pentyl chain, and [*m/z*] 187 and 159, indicating metabolic alteration at the naphthyl moiety.

Mass spectra of F02.3, detected six times, additionally contained [*m/z*] 249, 231 and 171, suggesting one monohydroxylation each at the naphthyl moiety and at the aliphatic side chain.

The F02.2 metabolites shared product ions with F02.3, in particular [*m/z*] 171 and 249, indicating monohydroxylation of the naphthyl moiety and a further monohydroxylation of the 1-(5F-pentyl)-1*H*-indazole moiety. As their mass spectra also contained [*m/z*] 229, 193, 161 and 133, the location of the second monohydroxylation was concluded to be at the indazole moiety.

Mass spectra of F02.4 metabolites shared [*m/z*] 193, 161 and 133 with those of the F02.2 type, indicating a monohydroxylation at the indazole moiety. The mass

spectra of F02.4 also shared product ions [*m/z*] 265, 155, and 127, relating to another monohydroxylation of the 5-fluoropentyl chain and to an unaltered naphthyl moiety. F02.4 was detected twice.

Trihydroxylation (F03)

Trihydroxylated species of THJ-2201 were screened by PIS with [*m/z*] 409 as the precursor ion. In total, five trihydroxylated metabolites could be detected in the pHLM incubation solution. F03.1 shared product ions [*m/z*] 187 and 159, indicating a dihydroxylation at the naphthyl moiety. Mass spectra also contained [*m/z*] 249, 231 and 145, suggesting a monohydroxylation at the 5-fluoropentyl chain and an unaltered indazole moiety.

Oxidative defluorination and further monohydroxylation (F04)

PIS for [m/z] 359 and 375 resulted in one and seven metabolites, respectively. PIS for [*m/z*] 359 yielded in the F04.1 metabolite, which is equivalent to the M01.3 metabolite (see Fig. 1), due to the oxidative defluorination of THJ-2201 (replacement of the fluorine by a hydroxyl group in the ω-position) leading to THJ-018 N-(5-OH-pentyl). The F04.1 metabolite was proven to be one of the main THJ-2201 metabolites.

Conducting PIS for [*m/z*] 375 resulted in the detection of seven metabolites, possibly due to the oxidative defluorination and further monohydroxylation—equivalent to some of the dihydroxylated THJ-018 metabolites (M02.2, M02.4, and M02.5).

In particular, the two F04.2 metabolites shared product ions with M02.5, but additionally contained [*m/z*] 229, probably due elimination of water from the hydroxylation of the ω-position during ESI fragmentation, leading to a double bond.

Furthermore, F04.3 shared all of the product ions with M02.4. The F04.3 was identified four times.

F04.4 and F04.2 shared almost all product ions, namely [m/z] 155 and 127, suggesting an unaltered naphthyl moiety, and [m/z] 247 and 229 according to a dihydroxylation of the 1-pentyl-1H-indazole moiety. By contrast, the mass spectrum of F04.4 showed [m/z] 145 due to an unaltered indazole moiety and, consequently, dihydroxylation of the aliphatic side chain.

Oxidative defluorination and further dihydroxylation (F05)

PIS for [m/z] 391 led to the identification of one F05.1 type metabolite. The mass spectrum of F05.1 shared [m/z] 231, 187, and 145 with the mass spectrum of M03.2. In addition, [m/z] 213 was observed, all indicating the 1-(5-OH-pentyl)-1H-indazole moiety and a dihydroxylation at the naphthyl moiety.

Formation of a quinone function and further hydroxylation (F06)

PIS for [m/z] 391 led to the identification of a metabolite with a quinone partial function at the naphthyl moiety. The mass spectrum of F06.1 contained product ions at [m/z] 213 and 145, indicating no alteration of the 1-(5F-pentyl)-1H-indazole moiety, and at [m/z] 185 and 157, suggesting a quinone partial structure at the naphthyl moiety. [m/z] 185 resulting from a neutral loss of hydrogen fluoride (− 18 Da) was excluded due to its inappropriate exact mass.

Two metabolites with a quinone partial structure at the naphthyl moiety and a further monohydroxylation could be identified due to PIS of [m/z] 407. The product ion mass spectra of F06.2 (see Fig. 5) contained [m/z] 233, 213 and 177 as well as [m/z] 145, suggesting the presence of an unmodified 1-(5F-pentyl)-1H-indazole moiety. The detection of [m/z] 201 and 173 confirmed a quinone

partial structure as well as a further monohydroxylation at the naphthyl moiety. This low abundance metabolite type has not been previously described.

Metabolic formation of a carboxylic acid and further hydroxylation (F07)

F07.1 was already assigned to the THJ-2201 N-pentanoic acid with a precursor molecule ion of [m/z] 373, as the metabolite is equivalent to the M04.3 metabolite due to oxidative defluorination and further oxidation, matching retention time (see Fig. 2) and product ions. However, the mass spectrum of F07.1 contained [m/z] 217, another characteristic fragment for the N-pentanoic acid, not observed for M04.3.

PIS of [m/z] 389 led to identification of two F07.2 metabolites. Neutral loss of formic acid (− 46 Da) led to a product ion at [m/z] 343. F07.2 shared the characteristic pentanoic acid fragments with F07.1—[m/z] 245 and 217—and additionally showed [m/z] 171 and 145, suggesting an unaltered indazole moiety and further monohydroxylation at the naphthyl moiety.

Formation of a dihydrodiol-function (F08)

As with M05.1 (THJ-018 dihydrodiol), the PIS of precursor ion [m/z] 395 confirmed the same metabolic reaction pathway for THJ-2201. Mass spectra of F08.1 shared [m/z] 189 and 145 with M05.1, but also showed [m/z] 233, 213, and 177, indicating an unaltered 1-(5F-pentyl)-1H-indazole moiety.

N-Desalkylation (F09)

As expected, results from PIS of precursor ion [m/z] 273 were in the accordance with the results for THJ-018 being the F09.1 metabolite identical with the M08.1 metabolite by matching retention time and mass spectrum.
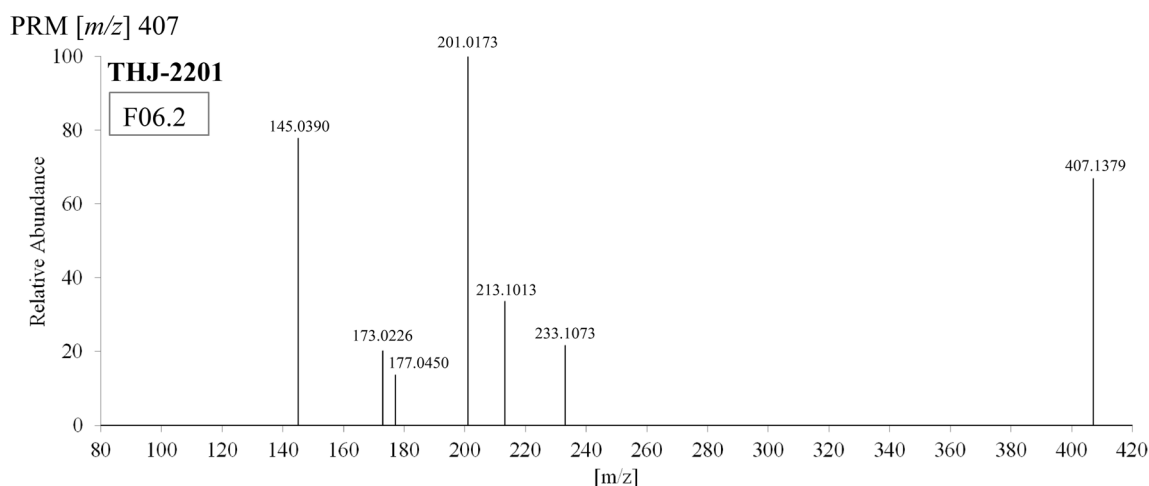

Fig. 5 HRMS spectrum of the THJ-2201 metabolite F06.2 in the parallel reaction monitoring (PRM) mode

Table 3 Detected THJ-2201 metabolites after pHLM and CYP incubation in comparison with metabolites from human urine samples and metabolites after incubation with human hepatocytes, as reported by Diao et al. (2015) (the three most abundant in vitro metabolites per assay are highlighted)

Metabolites			Metabolic reaction			Human urine (n=12)	pHLM	CYP								Human hepatocytes (abbreviations used in the reference) [16]
Group	Reaction	Abbreviation	i	a	n			1A2	2B6	2C9	2C19	2D6	2E1	3A4	3A5	
F01	OH	F01.1			OH	⊠ (n=10)	⊠	⊠	⊠	⊠	⊠	⊠	⊠	⊠	⊠	× (F13)
		F01.2	OH				×									
		F01.3		OH			×	⊠	⊠	⊠	⊠	⊠	⊠	⊠	⊠	× (F27)
F02	(OH)₂	F02.1			(OH)₂		×	×								× (F17, F20, F23)
		F02.2		OH	OH		×		×	×	×			×	×	
		F02.3		OH	OH	× (n=2)	×		×		×	×		×	×	
		F02.4		OH			×				×					
F03	(OH)₃	F03.1		OH	(OH)₂		×					×				
F04	Ox. (-HF) (+OH)	F04.1		Ox. (-HF)		⊠ (n=12)	⊠	⊠	⊠	⊠	⊠	⊠	⊠	⊠	×	⊠ (F26)
		F04.2	OH	Ox. (-HF)			×				×				×	
		F04.3		Ox. (-HF)	OH	⊠ (n=10)	⊠	×	×	×	×	×		×	⊠	× (F7)
		F04.4		Ox. (-HF) + OH			×		×							
F05	Ox. (-HF) +(OH)₂	F05.1		Ox. (-HF)	(OH)₂		×									
F06	quinone (+OH)	F06.1			quinone		×									
		F06.2			quinone + OH		×									
F07	COOH (+OH)	F07.1		COOH		× (n=10)	×	×	×		×			×	×	⊠ (F25)
		F07.2		COOH	OH	× (n=10)	×	×				×		×	×	⊠ (F2, F5, F10)
F08	dihydrodiol	F08.1			dihydrodiol	× (n=10)	×		×		×	×		×	×	× (F21)
F09	N-desalkylation	F09.1	N-desalkylation				×	×	×					×	×	× (F24)

i indazole moiety

a aliphatic side chain

n naphthyl moiety

OH monohydroxylation

(OH)₂ dihydroxylation

(OH)₃ trihydroxylation

C=O "carbonylation" (formation of a carbonyl function)

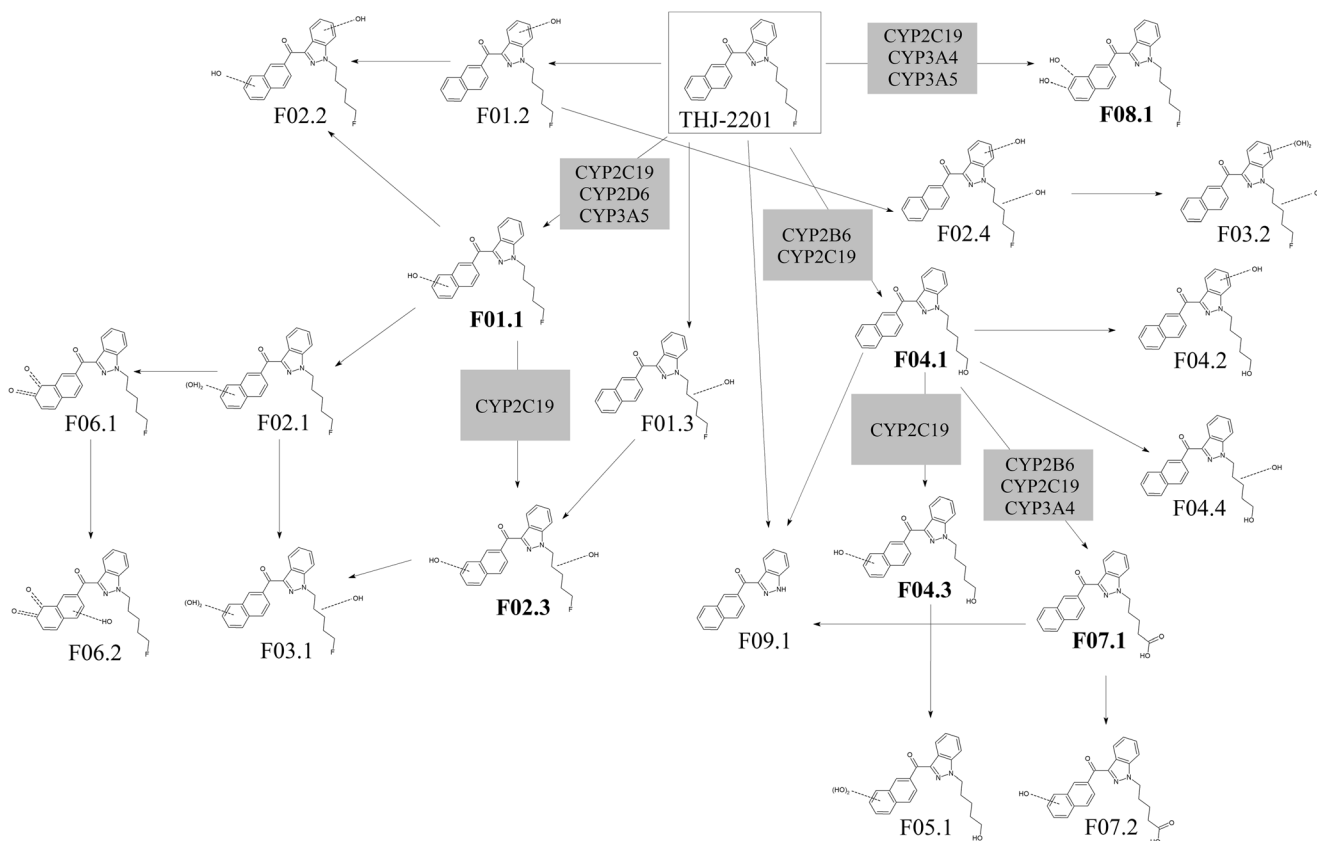COOH "carboxylation" (formation of the pentanoic acid)

Fig. 6 Postulated metabolic pathways of THJ-2201 after incubation with pHLM. Metabolite types detected in urine samples from THJ-2201 users are printed in bold type and labelled with the CYP isoforms that dominantly catalyzed the reactions

Metabolic pattern of THJ-2201 after incubation with CYPs

Results of CYP incubation with THJ-2201 were similar to those obtained for THJ-018 (see Supplementary Table 2). In total, the number of THJ-2201 metabolites detected after CYP incubation ranged between three (CYP2E1) and 11 (CYP2C19) metabolite types.

With respect to their summed metabolite peak abundancies, CYP2C19, CYP2B6, CYP3A5, and CYP3A4 were observed to contribute most to the microsomal metabolism of THJ-2201 (listed here in the order of relevance), followed by CYP2D6, CYP1A2 and CYP2C9. CYP2E1 made, by far, the lowest contribution.

Comparison of in vitro THJ-2201 metabolic patterns with in vivo metabolic patterns

Table 3 gives an overview of in vitro metabolic patterns of THJ-2201 obtained after pHLM, CYP and hepatocyte incubation as reported by Diao et al. (2016) [16] as well as of the in vivo metabolic patterns obtained via screening of 12 urine samples from proven THJ-2201 users. Figure 6 illustrates the metabolic pathways of THJ-2201.

Compared to Diao et al. (2015) [17], results were in good accordance, with the difference being that microsomal incubation yielded far more metabolites and shared only one main metabolite with hepatocyte incubation, namely F04.1 (oxidative defluorination), which was named F26 in the cited reference. This metabolite was found to be present in all of the 12 tested urine samples. In contrast to THJ-018, the main metabolites observed after microsomal incubation of THJ-2201 were also main metabolites observed in vivo.

Relevant in vivo metabolites could be observed with almost all of the in vitro models. However, F02.3, F04.3. F07.1, F07.2, and F08.1 were not observed after all of the conducted CYP incubations. Evaluation of the results showed that urinary metabolites were produced by various CYPs and that no metabolite is produced by a single CYP only. In addition, F02.3 was also not observed after hepatocyte incubation [17]. This is worth mentioning, as microsomal incubation generally generated further dihydroxylated and trihydroxylated metabolites, not observed by Diao et al. (2015) [17]. However, Diao et al. (2015) also described some further metabolites (the formation of an N-oxide at the indazole moiety, oxidative defluorination and dihydrodiol formation on the naphthyl residue, oxidative defluorination to the pentanoic acid and dihydrodiol formation on the naphthyl

moiety) [17], which were neither observed in vitro nor in vivo in this study.

Discussion

THJ-018 and THJ-2201 were shown to be extensively metabolized as pHLM and CYP in vitro incubation assays expressed a great variety of metabolites. Comparison of the results obtained from pHLM and CYP incubation along with published data obtained from hepatocyte incubation with those from urine screenings, showed that those in vitro models are all able to produce the relevant metabolites observed in vivo. However, CYP incubation or hepatocytes alone would not have been sufficient for the identification of all the THJ-018 and THJ-2201 metabolites detected in vivo. The F07.2 and F02.3 metabolite would both have been missed out with CYP incubation and with hepatocyte incubation, respectively. pHLM incubation, however, produced all the detected metabolites in urine. This may indicate some advantage in the production of phase I metabolites, which may not be present for other substances. The application of complementary methods did, however, advance knowledge of the metabolism of THJ-018 and THJ-2201.

When considering shared metabolites arising from oxidative defluorination and further oxidation of THJ-2201, the dehydrogenated THJ-018 metabolite (M07.1) and the monohydroxylated THJ-2201 metabolite (F01.1) should be used to substantiate positive urine samples. Although the THJ-2201 pentanoic acid (F07.1) was observed with higher abundance in comparison to the THJ-018 pentanoic acid (M04.3) in vitro, this metabolite should only be used with caution when making the distinction between THJ-018 and THJ-2201 intake.

All in vitro assays produced a variety of metabolites not detected in urine. As a substance-specific optimization of glucuronide cleavage was not possible, it cannot be fully excluded that some metabolites could have been missed out in urine.

Evaluation of the CYP incubation results suggested CYP2C19, CYP2B6, CYP3A4, and CYP3A5 being the relevant CYP isoforms in the metabolism of THJ-018 and THJ-2201 in vitro. The significance of CYP2C19 and CYP3A4 for the in vitro metabolism of synthetic cannabinoids has already been described for JWH-018, AM-2201 and AKB-48 by Chimalakonda et al. (2012) and Holm et al. (2015) [17, 18].

As their metabolism are distributed in several CYP isoforms, clinically relevant interactions with other drugs in suppressing significantly the metabolism of THJ-018 and THJ-2201 can be expected to be of non-impact.

Conclusion

pHLM, CYP as well as hepatocyte approaches were proven to be useful and complementary tools in revealing the metabolism

of THJ-018 and THJ-2201 and in finding appropriate targets for urine screening—in particular, for their differentiation. In addition, with CYP assays, the most relevant CYP isoforms involved in metabolism can be identified. When looking at phase I metabolites detected in urine, results from hepatocyte, pHLM and CYP incubation are very similar, with the advantage that CYP and pHLM assays do not require cell culture knowledge and equipment. However, hepatocytes provide the additional opportunity to identify a broad range of phase II metabolites. For a comprehensive study of the metabolism of a substance, the use of complementary methods is advised. Substances that are being tested for, and that share some metabolites, drive the requirement for a substance-specific metabolite to be incorporated in the screening process, e.g., the monohydroxylated THJ-2201 metabolite (F01.1) and the dehydrogenated THJ-018 metabolite (M07.1).

Compliance with ethical standards

Compliance with the law All experiments comply with the current laws of the Federal Republic of Germany.

Conflict of interest The authors declare that they have no conflict of interest.

Publisher's note Springer Nature remains neutral with regard to jurisdictional claims in published maps and institutional affiliations.

References

1. Castaneto MS, Wohlfarth A, Desrosiers NA, Hartman RL, Gorelick DA, Huestis MA (2015) Synthetic cannabinoids pharmacokinetics and detection methods in biological matrices. Drug Metab Rev 47(2):124–174. https://doi.org/10.3109/03602532.2015.1029635
2. Wintermeyer A, Möller I, Thevis M, Jübner M, Beike J, Rothschild MA, Bender K (2010) In vitro phase I metabolism of the synthetic cannabimimetic JWH-018. Anal Bioanal Chem 398(5):2141–2153. https://doi.org/10.1007/s00216-010-4171-0
3. Sobolevsky T, Prasolov I, Rodchenkov G (2012) Detection of urinary metabolites of AM-2201 and UR-144, two novel synthetic cannabinoids. Drug Test Anal 4(10):745–753. https://doi.org/10.1002/dta.1418
4. Chimalakonda KC, Seely KA, Bratton SM, Brents LK, Moran CL, Endres GW, James LP, Hollenberg PF, Prather PL, Radominska-Pandya A, Moran JH (2012) Cytochrome P450-mediated oxidative metabolism of abused synthetic cannabinoids found in K2/Spice: identification of novel cannabinoid receptor ligands. Drug Metab

Dispos 40(11):2174–2184. https://doi.org/10.1124/dmd.112.047530

5. Chimalakonda KC, Moran CL, Kennedy PD, Endres GW, Uzieblo A, Dobrowolski PJ, Fifer EK, Lapoint J, Nelson LS, Hoffman RS, James LP, Radominska-Pandya A, Moran JH (2011) Solid-phase extraction and quantitative measurement of omega and omega-1 metabolites of JWH-018 and JWH-073 in human urine. Anal Chem 83(16):6381–6388. https://doi.org/10.1021/ac201377m

6. Möller I, Wintermeyer A, Bender K, Jübner M, Thomas A, Krug O, Schänzer W, Thevis M (2011) Screening for the synthetic cannabinoid JWH-018 and its major metabolites in human doping controls. Drug Test Anal 3(9):609–620. https://doi.org/10.1002/dta.158

7. Hutter M, Broecker S, Kneisel S, Auwärter V (2012) Identification of the major urinary metabolites in man of seven synthetic cannabinoids of the aminoalkylindole type present as adulterants in 'herbal mixtures' using LC-MS/MS techniques. J Mass Spectrom 47(1):54–65. https://doi.org/10.1002/jms.2026

8. Hutter M, Moosmann B, Kneisel S, Auwärter V (2013) Characteristics of the designer drug and synthetic cannabinoid receptor agonist AM-2201 regarding its chemistry and metabolism. J Mass Spectrom 48(7):885–894. https://doi.org/10.1002/jms.3229

9. Kröner L, Spencer VC (2013) A pragmatic approach to detect SPICE-metabolites in urine with HPLC-MS/MS. Toxichem Krimtech 80:375–380

10. Moonhee J, Wonkyung Y, Hyeyoung C, Heyejin C, Sooyeun L, Eunmi K, Heesun C (2013) Monitoring of urinary metabolites of JWH-018 and JWH-073 in legal cases. Forensic Sci Int 231(1–3):13–19. https://doi.org/10.1016/j.forsciint.2013.03.053

11. Wohlfarth A, Scheidweiler KB, Castaneto M, Gandhi AS, Desrosiers NA, Klette KL, Martin TM, Huestis MA (2014) Urinary prevalence, metabolite detection rates, temporal patterns and evaluation of suitable LC-MS/MS targets to document synthetic cannabinoid intake in US military urine specimens. Clin Chem Lab Med 53(3):423–434. https://doi.org/10.1515/cclm-2014-0612

12. Moonhee J, Wonkyung Y, Shin I, Hyeyoung C, Heyejin C, Eunmi K (2014) Determination of AM-2201 metabolites in urine and comparison with JWH-018 abuse. Int J Legal Med 128(2):285–294. https://doi.org/10.1007/s00414-013-0884-x

13. Scheidweiler KB, Huestis MA (2014) Simultaneous quantification of 20 synthetic cannabinoids and 21 metabolites, and semi-quantification of 12 alkyl hydroxy metabolites in human urine by liquid chromatography-tandem mass spectrometry. J Chromatogr A 1327:105–117. https://doi.org/10.1016/j.chroma.2013.12.067

14. Scheidweiler KB, Jarvis MJ, Huestis MA (2015) Nontargeted SWATH acquisition for identifying 47 synthetic cannabinoid metabolites in human urine by liquid chromatography-high-resolution tandem mass spectrometry. Anal Bioanal Chem 407(3):883–897. https://doi.org/10.1007/s00216-014-8118-8

15. Watanabe S, Kuzhiumparambil U, Winiarski Z, Fu S (2016) Biotransformation of synthetic cannabinoids JWH-018, JWH-073 and AM2201 by Cunninghamella elegans. Forensic Sci Int 261:33–42. https://doi.org/10.1016/j.forsciint.2015.12.023

16. Diao X, Wohlfarth A, Pang S, Scheidweiler KB, Huestis MA (2015) High-resolution mass spectrometry for characterizing the metabolism of synthetic cannabinoid THJ-018 and its 5-Fluoro analog THJ-2201 after incubation in human hepatocytes. Clin Chem Lab Med 62(1):1–13. https://doi.org/10.1373/clinchem.2015.243535

17. Fietzke M, Thomas A, Beike J, Rothschild MA, Thevis M, Mercer-Chalmers-Bender K (2016) In vitro elucidation of the metabolic profile of the synthetic cannabinoid receptor agonists JWH-175 and JWH-176. Forensic Toxicol 34(2):353–362. https://doi.org/10.1007/s11419-016-0322-0

18. Peters FT (2014) Recent developments in urinalysis of metabolites of new psychoactive substances using LC–MS. Bioanalysis 6(15):2083–2107